U.S. DEPARTMENT OF COMMERCE
NATIONAL OCEANIC AND ATMOSPHERIC ADMINISTRATION
NATIONAL WEATHER SERVICE
NATIONAL METEOROLOGICAL CENTER

OFFICE NOTE 196

Simulation Experiments of Surface Pressure Analyses with Optimum Interpolation

Tsann-wang Yu
Doris Gordon
Development Division

JANUARY 1979

Simulation Experiments of Surface Pressure Analyses with Optimum Interpolation

1. Introduction

Scatterometer-derived data from the SEASAT-A satellite will provide fine resolution surface wind vectors over the ocean. Presumably, these data may improve the surface pressure analyses currently generated by sparsely available ship reports. The improved surface pressure analysis may also be included in a global data assimilation system in NMC (McPherson et al., 1979).

While awaiting the arrival of the SEASAT-A wind data, we have decided to run a series of simulation experiments on surface pressure analyses using conventional ship wind and pressure reports. The main purpose of these experiments is to study the effect of ship wind data on surface-pressure analyses. It is anticipated that results of this study might supply information on the potential impact of the SEASAT-A wind data.

This paper describes results of the simulation experiments on surface pressure analyses by a modified version of the optimum interpolation scheme currently operational in NMC (Bergman, 1979). It should be pointed out that Druyan (1972) has performed similar experiments using a boundary layer model of Cardone (1969) for calculating surface pressures. He concluded that ship winds contribute substantially to the specification of sea level pressure. Since we are mainly interested in large-scale synoptic pressure waves, we used an experimental design different from that of Druyan (1972). Section 2 discusses the details of the design. Test results are presented in Section 3; and in Section 4, a brief concluding remark is given.

2. Experimental Design

Two basic experiments are in order. The first experiment is designed for a limited oceanic region, e.g., between 310°E and 330°E in longitude, and between 25°N and 45°N in latitude. Over this limited Atlantic ocean region, there are approximately 20 ship reports at any synoptic time. The second experiment is designed for a global region within a latitude belt of 25°N and 45°N. Over this global region, there are approximately 300 ship reports and about 2000 surface pressure observations over the land surfaces. The limited oceanic region analysis experiment enables one to monitor the input data because of the limited number of observations. The global analysis experiment, on the other hand, enables us to perform Fourier analysis of the pressure waves--thereby one may study the spectrum distribution of the pressure waves.

With the optimum interpolation (hereafter referred to as OI) scheme, we may readily analyze surface pressure by either using surface pressure data alone (this constitutes the so-called univariate pressure analysis) or using both pressure and wind data (multivariate p analysis).

Differences in results from these two analyses should reveal an effect of wind data on surface pressure analysis. Moreover, it is conceivable that if surface pressure observations alone were gradually deleted, the OI scheme would tend to place more emphasis on wind data. This led us to conduct a series of simulations in which certain portions of pressure data were withheld and only the ship wind observations were used. This should enhance the detection of the effect of wind data on surface pressure waves.

A. Atlantic Ocean regional analysis

The distribution of ship locations for November 24, 0000 GMT 1978 for the limited region is shown in Fig. 1. A 2.5° by 2.5° longitude-latitude grid consistent with the NMC global operational analysis system is used for analyzing the surface pressure. As pointed out previously, for the limited number of ship reports, we may readily control the deletion of pressure data. Table 1 summarizes eight simulation runs with various data bases.

Table 1: Ship Wind and Pressure Data Points Used for the Limited Region Analysis

Run	Types of Analyses	No. of Pressure Data	No. of Wind Data	Locations of Data Points in Figure 1
A1	Univariate	19	0	All pressure data
A2	Multivariate	19	19	All pressure and wind
A3	Multivariate	9	19	2,4,6,8,10,12,14,16,18
A4	Multivariate	5	19	1,5,9,13,17
A5	Multivariate	3	19	1,9,17
A6	Univariate	9	0	Same as A3
A7	Univariate	5	0	Same as A4
A8	Univariate	3	0	Same as A5

B. Global analysis between 25°N and 45°N

The design for a series of simulation runs of global pressure analysis is conceptually similar to that of the limited region. The main difference lies in that we are dealing with a global region which contains many more ship wind and pressure observations. Moreover, many surface pressures from land stations are used. Consequently, the process of deleting pressure observations deserves mention. First, we sorted out all the pressure data in 1° latitude belt and selected every other one or every other two (and so forth) pressure observations in that latitude belt. Second, we would proceed the same way in the longitude direction. For example, if we selected every other pressure data in a 1° latitude belt, followed by a selection of every other pressure data in a 1° longitude band, this would constitute a case where only 25% of total pressure data is used. Table 2 summarizes details of simulation runs for the global analysis.

Table 2: Various Data Bases Used in the Global Pressure Analysis

Run	Type of Analysis	No. of Pressure Data	No. of Wind Data
B1	Univariate	100%	0
B2	Multivariate	100%	100%
B3	Multivariate	25%	100%
B4	Multivariate	11%	100%
B5	Multivariate	6%	100%
B6	Univariate	25%	0%
B7	Univariate	11%	0%
B8	Univariate	6%	0%

It should be pointed out that in all the experiments, we set a first guess pressure field to be 1013.2 mb and a first guess wind field to be u=0 and v=0. This may be justified because we are mainly interested in the comparative performances of each run. That is, the pressure analysis generated by Run B1 (see Table 2, i.e., 100% univariate p analysis) is the standard against which surface pressure fields generated by using a lower data density are compared. Thus, we contend that errors that might be incurred by the first guess fields of pressure and wind should not affect our final conclusions.

3. Discussions

B. Results of the Atlantic Ocean regional analysis

The RMS (root mean square) pressure differences between the fields generated at lower data density and the univariate pressure analysis generated by using all the data (Run A1) were computed. In addition, analyzed surface pressures for each data base were correlated with the pressures of Run A1 and correlation coefficients calculated. These results are shown in Table 3. We see that the addition of all ship wind data changes

Table 3: RMS Pressure Differences and Correlation Coefficients Computed for Various Similation Runs With Respect to Run A1.

Runs	A2	A3	A4	A5	A6	A7	A8
RMS Pressure Differences (mb)	1.555	1.972	3.016	4.843	2.267	3.825	4.727
Correlation Coefficients	.965	.950	.887	.783	.947	.802	.805

the surface pressure by an amount of 1.555 mb in RMS difference (see Run A2 in Table 3). As expected, the RMS pressure differences increase as additional pressure data are withheld from the analysis. For example, when the pressure observations are reduced to about 50% of the maximum pressure observations (see Run A3), the RMS differences increase to be 1.972 mb. When the pressure data are reduced to about 25% of the total (Run A4), the RMS pressure differences increase to be 3.016 mb.

From Table 3, we can also see the effect of wind data on the surface pressure. Referring to Table 2, Runs A3, A4 and A5 are based on analyses using wind data while Runs A6, A7 and A8 are analyses without wind data. We see that when pressure data are decreased by 50%, inclusion of wind data contributes about 0.3 mb in RMS pressure differences (compare Runs A3 and A6). As pressure data are further reduced to about 25% of the total, inclusion of wind data contributes about 0.8 mb in RMS pressure difference (compare Run A4 and A7). However, when we select only 3 pressure observations out of 19 data points, the wind data apparently makes no impact on the surface pressure analysis (compare Runs A5 and A8).

The correlation coefficients calculated for each run, with respect to Run A1, are also shown in Table 3. Consistent with RMS pressure differences, the correlation coefficients decrease as more pressure data are deleted.

B. Results of global analysis between 25°N and 45°N

Two synoptic times were chosen for the simulation experiments, i.e., Case 1 : Oct. 1, 1200 GMT, 1978 and Case 2 : Oct. 27, 1200 GMT, 1978. As previously mentioned, there were typically about 300 ship reports and about 2000 surface pressure observations within the belt of 25°N and 45°N.

As in the limited regional analysis experiments, we calculated RMS pressure differences for the whole global region with various data bases as shown in Table 2. We also calculated RMS pressure differences for four small regions: Region I, Atlantic Ocean region (15°W - 70°W); Region II, Pacific Ocean region (145°E - 225°E); Region III, U.S. Continental region, (70°W - 125°W); and Region IV, the Mass Continental region (0°E - 145°E and 0° - 15°W).

Table 4 shows RMS pressure differences calculated for various simulation experiments of the global pressure analysis. Again, results of Run B1 (i.e., 100% univariate pressure analysis, Table 2) are the comparison standard. We see from Table 4 that RMS pressure differences increase as more pressure data are withheld from the analysis. This is consistent with the results of Regional Atlantic Ocean simulation experiments as discussed previously. We see that using 100% pressure data, addition of wind data contributes a 0.421 mb in RMS pressure differences in the whole global region for Case 1 . When we use only 25% pressure data, the RMS pressure differences increase to be 1.725 mb (see Run B3 in Table 4a). Further reduction of the pressure data to 6% of the total increases RMS pressure differences to 2.859 mb (see Run B5).

Table 4: RMS Pressure Differences Calculated With Respect to Run B1 for Various Simulation Experiments

(a) Case 1: Oct. 1, 1978 1200 GMT

Experiment Run	B1	B2	B3	B4	B5	B6	B7	B8
Global Region	-	.421	1.725	2.206	2.859	1.726	2.259	2.967
Region I	-	.411	2.714	3.201	3.802	2.456	3.388	3.715
Region II	-	.769	1.943	2.655	4.140	2.147	2.717	4.490
Region III	-	.022	.696	1.385	1.018	0.699	1.317	0.964
Region IV	-	0.	1.252	1.600	1.721	1.252	1.596	1.724

(b) Case 2: Oct. 27, 1978 1200 GMT

Experiment Run	B1	B2	B3	B4	B5	B6	B7	B8
Global Region	-	.713	2.028	2.467	3.045	2.220	2.667	3.124
Region I	-	.248	2.101	1.996	2.770	2.465	1.951	3.287
Region II	-	1.396	2.412	3.306	3.599	2.809	3.885	3.603
Region III	-	.058	.959	1.219	1.769	1.007	1.168	1.713
Region IV	-	.033	2.097	2.455	3.186	2.102	2.461	3.176

The effect of ship wind data on the surface pressure analysis can be seen from comparing results of Runs B6, B7 and B8 with those of Runs B3, B4 and B5 respectively. For example, with 25% of the total pressure data, inclusion of ship wind data (Run B6) has a RMS pressure difference of 1.726 mb. This is to be compared with a RMS pressure difference of 1.725 mb without use of any wind data (Run B3). Thus, we see the effect of wind data on pressure field for Case 1 is negligible in the global region. This is also true for Case 1 when 11% (comparing Run B4 with B7) or 6% (comparing Run B5 with Run B8) of the total pressure data were used.

For Region I (Atlantic Ocean region), comparison of RMS pressure differences for Case 1 shows that ship wind data has little positive effect on the pressure field. In fact, inclusion of wind data causes a slight degradation of the pressure field. For Region II (Pacific Ocean region), ship wind data show to have a small positive impact on the pressure field for Case 1 .

The RMS pressure differences computed for Case 2 are shown in Table 4b. With the exception of the continental regions, addition of ship wind data does contribute positively in improving the pressure fields. This can be seen from comparing results of Runs B6, B7 and B8 with those of Run B3, B4 and B5 respectively in Table 4b.

The correlation coefficients calculated for the global analysis experiments are shown in Table 5a and Table 5b for Case 1 and Case 2 respectively. Consistent with the RMS pressure differences, the correlation

Table 5: Correlation Coefficients Calculated With Respect to Run B1 for Various Simulation Experiments

(a) Case 1: Oct. 1, 1978 1200 GMT

Experiment Run	B1	B2	B3	B4	B5	B6	B7	B8
Global Region	-	.998	.963	.945	.908	.962	.942	.896
Region I	-	.996	.896	.866	.868	.908	.821	.833
Region II	-	.989	.911	.837	.654	.888	.824	.540
Region III	-	1.000	.971	.867	.931	.971	.880	.940
Region IV	-	1.000	.973	.959	.949	.973	.959	.949

(b) Case 2: Oct. 27, 1978 1200 GMT

Experiment Run	B1	B2	B3	B4	B5	B6	B7	B8
Global Region	-	.995	.961	.944	.921	.953	.934	.919
Region I	-	.999	.931	.944	.909	.903	.952	.869
Region II	-	.948	.830	.771	.740	.752	.620	.732
Region III	-	1.000	.934	.892	.813	.927	.906	.825
Region IV	-	1.000	.978	.970	.950	.978	.970	.951

coefficients decrease as more pressure data are deleted. The substantial effect of wind data on pressure fields can be clearly seen from comparing the correlation coefficient values of Runs B6, B7 and B8 with those of Runs B3, B4 and B5.

To see differences in the energy distribution due to use of different data bases, we further performed a Fourier analysis (Gerrity, 1978) on each analyzed pressure field. Fig. 2 shows a result of the spectral analysis for Run B1 for Cases 1 and 2 . The horizontal axis is Fourier component or wave number, and the vertical axis is amplitude of the pressure waves. From Fig. 1 we see that most energy is contained in the large scale waves or small Fourier numbers. At Fourier number 24, the amplitude of the pressure waves decreases to nearly zero.

Differences in the spectral distribution due to use of different data bases are exhibited in Fig. 3. Since the spectral distribution of Case 1 is very similar to that of Case 2 , we shall not show results of Case 1 . Note that the vertical axis of Fig. 3 is in terms of normalized amplitudes with respect to those of Run B1. Thus, values greater than 1 indicate that amplitudes calculated by a field are greater than those of Run B1. For example, Curve B2 in Fig. 3 (corresponding to Run B2) shows that at small Fourier numbers, the amplitudes of Run B1 are nearly the same as those of Run B2. At large Fourier numbers, however, the amplitudes of Run B2 are greater than those of Run B1. This suggests that inclusion of ship wind data mainly leads to an increase in energy for small scale waves.

As pointed out previously, when the pressure data is gradually deleted, the OI system tends to place more weight on the wind data. This effect can be seen from Curves B3, B4 and B5 (corresponding to Runs B3, B4 and B5 respectively) in Fig. 3. We see that the ship wind data, in addition to contributing to the small scale wave phenomena, adds significantly to the large scale waves. The contributions by the wind data to the large scale waves are much smaller than those to the small scales.

To further illustrate the contributions by ship wind data, we calculated pressure amplitude ratios between pressure fields with wind data and those without wind data. The ratios calculated for various data bases are shown in Fig. 4. For example, Curve 2 shows the ratio of pressure amplitudes between Run B3 (with wind data) and Run B6 (without wind data). It clearly shows from Curve 2 that contribution due to wind data is mostly in the small scale waves. When more pressure data are deleted, this phenomenon becomes much more pronounced. This can be seen from Curves 3 (11% of total pressure) and Curve 4 (6% of the total pressure data) in Fig. 4.

4. Concluding Remarks

We conclude from this study that ship wind data contributes mostly to the small scale wave phenomena, although there is some evidence that wind data will add to the large scale pressure waves. The 2.5^{o} by 2.5^{o} longitude-latitude grid adopted for this study may be too coarse to resolve small scale features. Consequently, the RMS statistics from this study do not show conclusively that wind data improve pressure analyses for synoptic scale features.

Based on this study, it would appear desirable to design an experiment with a smaller grid system (i.e., 1^{o} longitude-latitude grid) for testing the impact of upcoming SEASAT-A scatterometer wind data. It is expected that the fine-resolution SEASAT wind data will contribute to the resolution of small scale features. But it awaits to be demonstrated that SEASAT-A wind data may add significantly to the synoptic scale pressure waves. We have thus far received two partial orbits of the SEASAT-A wind data and now testing the data with a similar surface pressure analysis experiment as described in this study. Results of these experiments will be reported later.

References

Bergman, K. H., 1979: Multivariate analysis of temperatures and winds using optimum interpolation. Submitted to Mon. Wea. Rev.

Cardone, V., 1969: Specification of wind distribution in the marine boundary layer for wave forecasting. CSL Report TR-69-1, Dept. of meteorology and Oceanography, New York University, 131 pages.

Druyan, L. M., 1972: Objective analysis of sea-level winds and pressures derived from simulated observations of a satellite radar-radiometer and actual conventional data. J. Appl. Meteor., 11, 413-428.

Gerrity, J. P., 1979: A partial diagnostic analysis of 7L PE output. NMC Office Note 172, 26 pages.

McPherson, R. M., K. H. Bergman, R. E. Kistler, G. E. Rasch, and D. S. Gordon, 1979: The NMC global data assimilation system. Submitted to Mon. Wea. Rev. Rev.

Acknowledgments

The authors would like to express their sincere thanks to K. H. Bergman, J. Gerrity, and R. M. McPherson for their helpful discussions during the course of this study. Their thanks also go to T. Krzenski for drafting the figures and T. East for typing the paper.

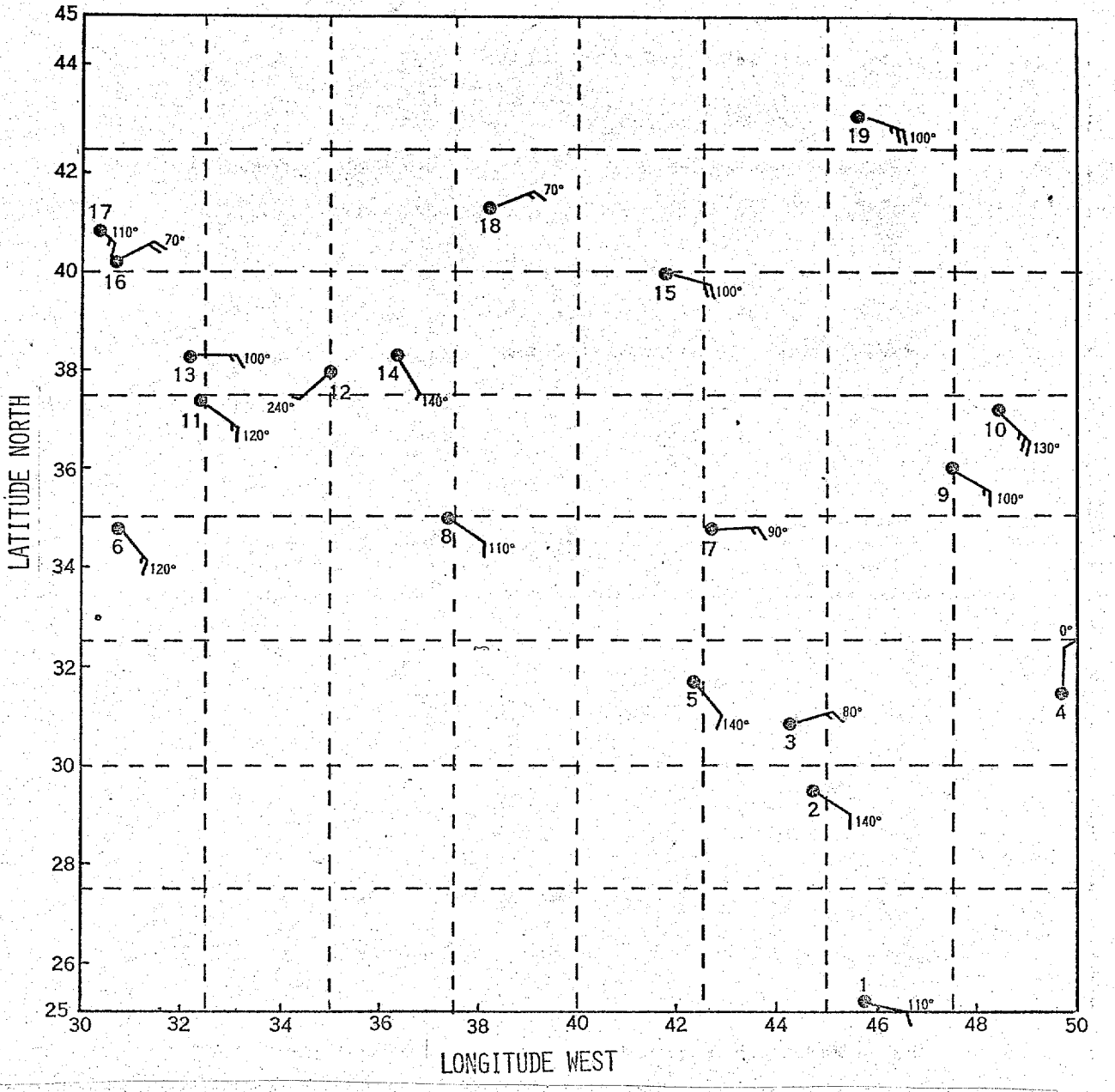

Fig. 1 Distribution of ship locations for November 24, 0000 GMT 1978. The order of data points is indicated numerically in the figure. The dotted lines represent a 2.5° by 2.5° longitude-latitude grid consistent with the NMC global operational analysis system.

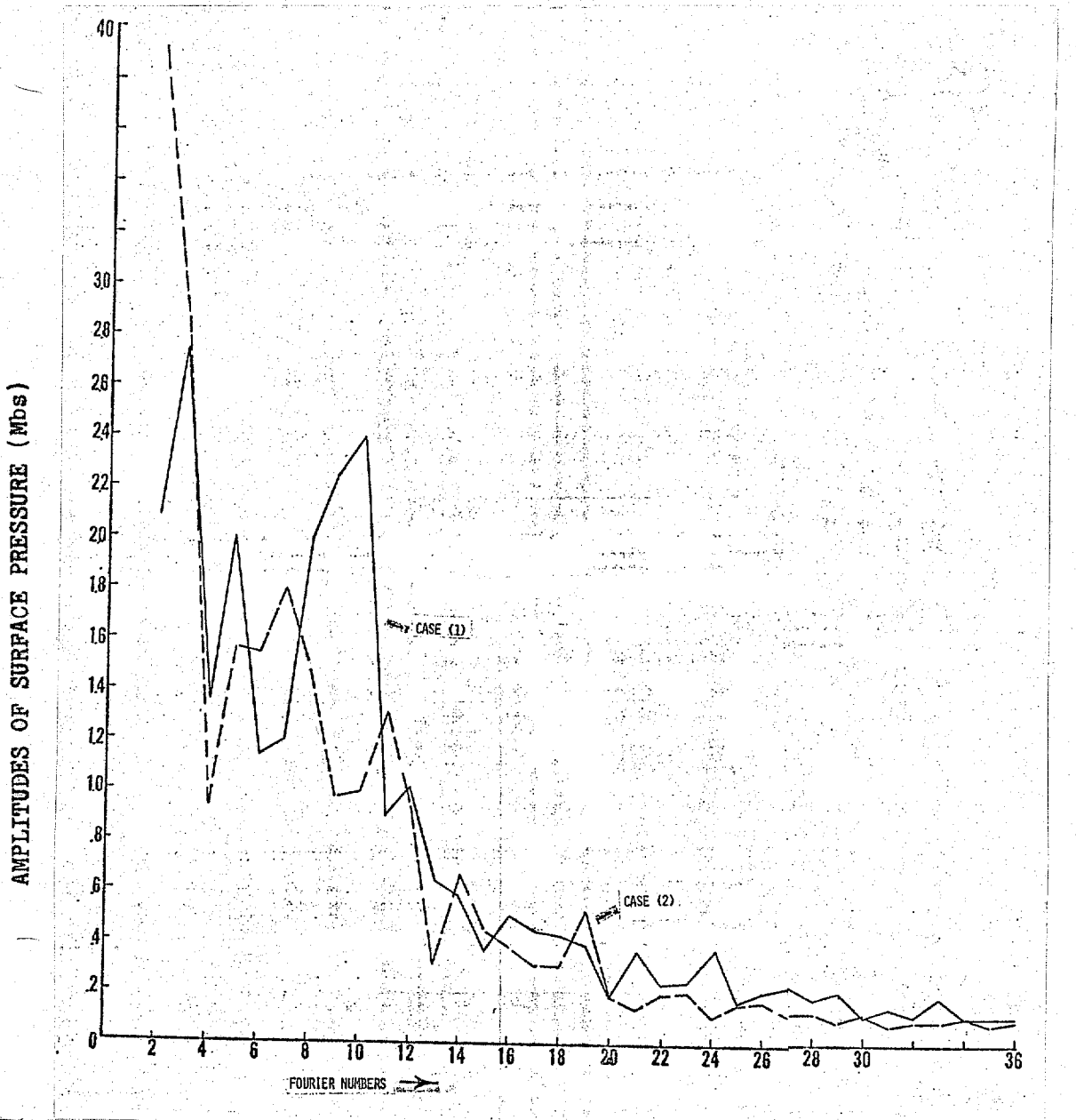

Fig. 2 Spectral distribution of surface pressure analyses for Case 1 (solid line) and Case 2 (broken line).

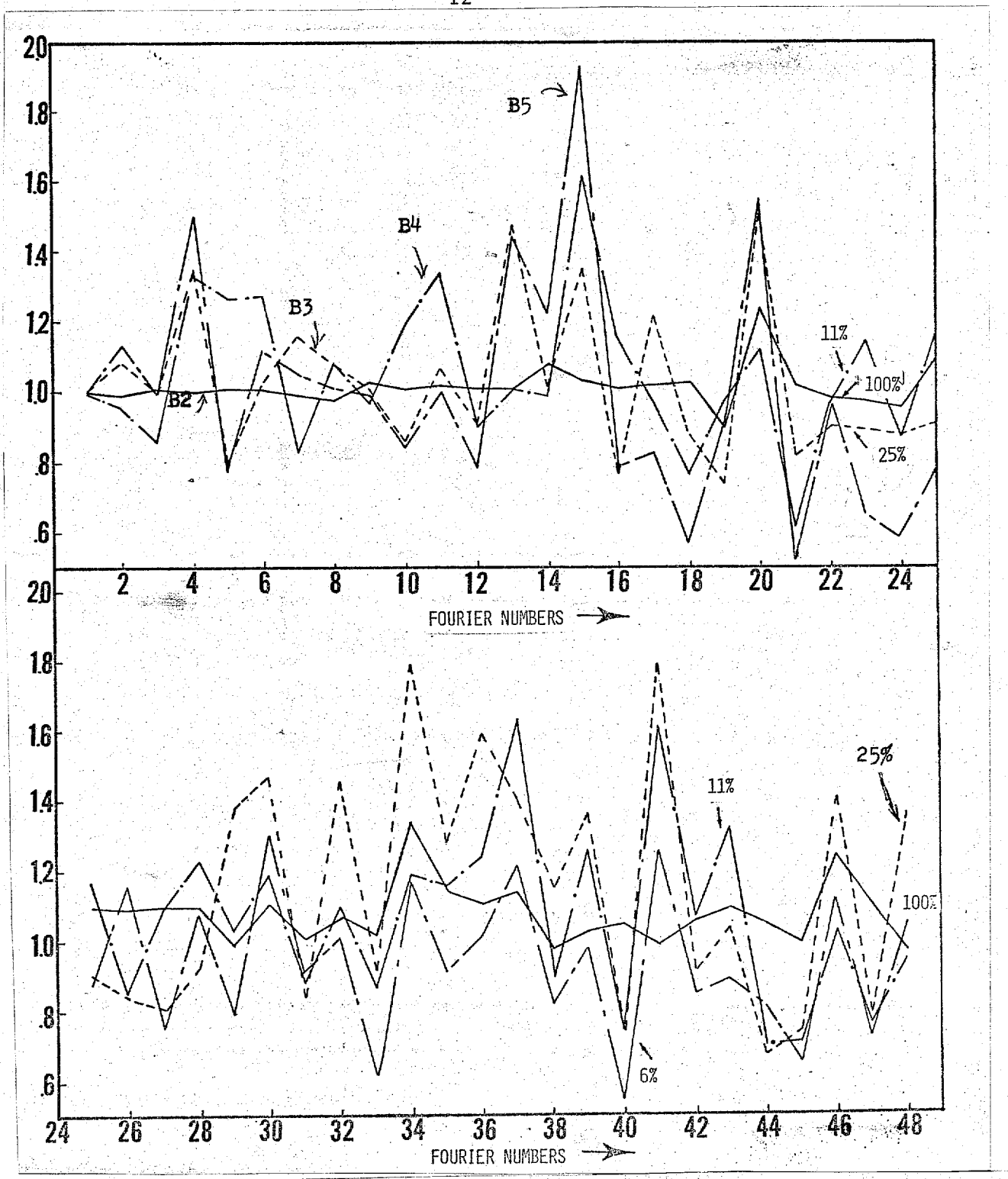

Fig. 3 Normalized pressure amplitudes calculated with respect to Run B1 (100% pressure data, univariate analysis). Percentage values of each curve indicate amounts of pressure data used in the analysis.

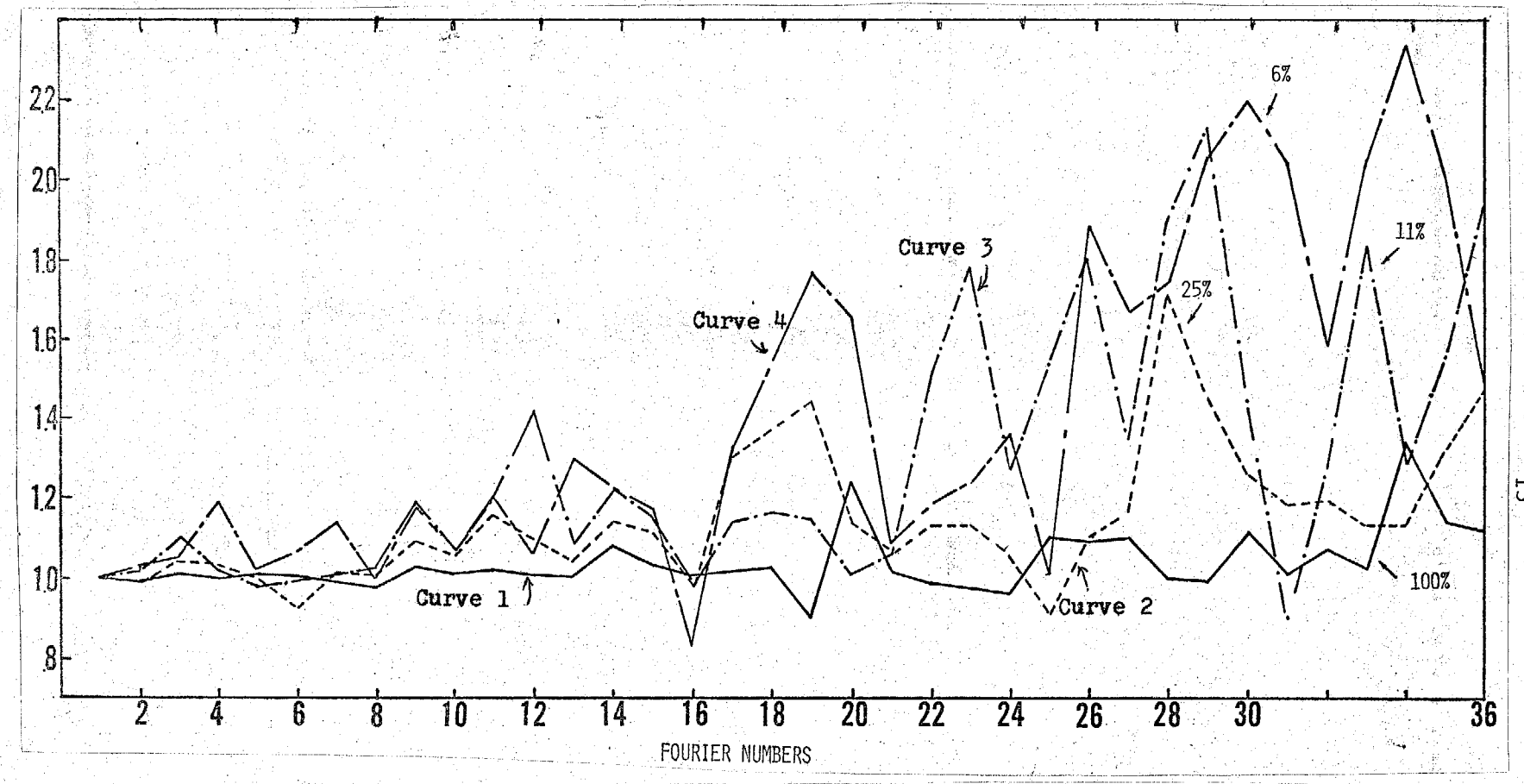

Fig. 4 Surface pressure amplitude ratios between analyses with wind data and those without wind data. Percentage values of each curve indicate amounts of pressure data used in the analysis.